**Natural Hazards
and Earth
System Sciences**

Great earthquakes along the Western United States continental margin: implications for hazards, stratigraphy and turbidite lithology

C. H. Nelson[1]**, J. Gutiérrez Pastor**[1]**, C. Goldfinger**[2]**, and C. Escutia**[1]

[1]Instituto Andaluz de Ciencias de la Tierra, Av. de las Palmeras, 4 18100 Armilla (Granada), Spain
[2]College of Oceanic and Atmospheric Sciences, Oregon State University, Corvallis OR 97331, USA

Correspondence to: C. H. Nelson (hansnelsonugr@hotmail.com) and C. Goldfinger (gold@coas.oregonstate.edu)

Abstract. We summarize the importance of great earthquakes ($M_\mathrm{w} \gtrsim 8$) for hazards, stratigraphy of basin floors, and turbidite lithology along the active tectonic continental margins of the Cascadia subduction zone and the northern San Andreas Transform Fault by utilizing studies of swath bathymetry visual core descriptions, grain size analysis, X-ray radiographs and physical properties. Recurrence times of Holocene turbidites as proxies for earthquakes on the Cascadia and northern California margins are analyzed using two methods: (1) radiometric dating (^{14}C method), and (2) relative dating, using hemipelagic sediment thickness and sedimentation rates (H method). The H method provides (1) the best estimate of minimum recurrence times, which are the most important for seismic hazards risk analysis, and (2) the most complete dataset of recurrence times, which shows a normal distribution pattern for paleoseismic turbidite frequencies. We observe that, on these tectonically active continental margins, during the sea-level highstand of Holocene time, triggering of turbidity currents is controlled dominantly by earthquakes, and paleoseismic turbidites have an average recurrence time of ~ 550 yr in northern Cascadia Basin and ~ 200 yr along northern California margin. The minimum recurrence times for great earthquakes are approximately 300 yr for the Cascadia subduction zone and 130 yr for the northern San Andreas Fault, which indicates both fault systems are in (Cascadia) or very close (San Andreas) to the early window for another great earthquake.

On active tectonic margins with great earthquakes, the volumes of mass transport deposits (MTDs) are limited on basin floors along the margins. The maximum run-out distances of MTD sheets across abyssal-basin floors along active

margins are an order of magnitude less (~ 100 km) than on passive margins (~ 1000 km). The great earthquakes along the Cascadia and northern California margins cause seismic strengthening of the sediment, which results in a margin stratigraphy of minor MTDs compared to the turbidite-system deposits. In contrast, the MTDs and turbidites are equally intermixed on basin floors along passive margins with a mud-rich continental slope, such as the northern Gulf of Mexico.

Great earthquakes also result in characteristic seismo-turbidite lithology. Along the Cascadia margin, the number and character of multiple coarse pulses for correlative individual turbidites generally remain constant both upstream and downstream in different channel systems for 600 km along the margin. This suggests that the earthquake shaking or aftershock signature is normally preserved, for the stronger ($M_\mathrm{w} \geq 9$) Cascadia earthquakes. In contrast, the generally weaker ($M_\mathrm{w} =$ or < 8) California earthquakes result in upstream simple fining-up turbidites in single tributary canyons and channels; however, downstream mainly stacked turbidites result from synchronously triggered multiple turbidity currents that deposit in channels below confluences of the tributaries. Consequently, both downstream channel confluences and the strongest ($M_\mathrm{w} \geq 9$) great earthquakes contribute to multi-pulsed and stacked turbidites that are typical for seismo-turbidites generated by a single great earthquake. Earthquake triggering and multi-pulsed or stacked turbidites also become an alternative explanation for amalgamated turbidite beds in active tectonic margins, in addition to other classic explanations. The sedimentologic characteristics of turbidites triggered by great earthquakes along the Cascadia
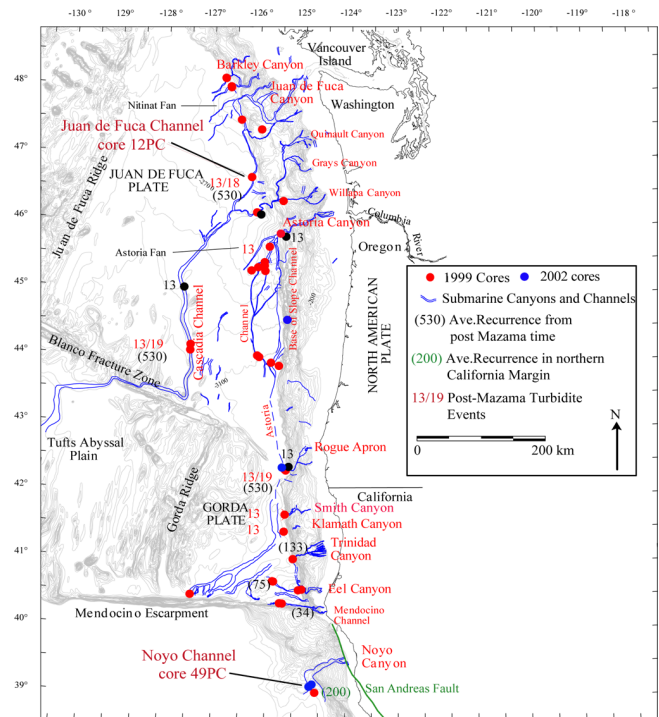
and northern California margins provide criteria to help distinguish seismo-turbidites in other active tectonic margins.

1 Introduction

In recent years, assessments based on turbidite characteristics have emerged as a useful tool for paleoseismic research (Goldfinger, 2011). As opposed to most onshore paleoseismic records, marine archives offer the potential of good preservation, good spatial coverage, and long temporal span. Turbidite frequency has been used to compile paleoseismologic records along seismically hazardous continental margins to reveal earthquake recurrence intervals on centennial to millennial time scales. Turbidite paleoseismology has been attempted in marine settings such as the Cascadian margin (Adams, 1990; Nelson et al., 2000; Goldfinger et al., 2003a, b, 2007, 2008, 2012; Gutiérrez Pastor et al., 2009), the northern California margin (Goldfinger et al., 2007, 2008; Gutiérrez Pastor et al., 2009), the southern California Borderland (Gorsline et al., 2000), Taiwan (Huh et al., 2004), Japan (Nakajima and Kanai, 2000; Noda et al., 2008), the Mediterranean Sea (Anastasakis and Piper, 1991; Kastens, 1984), the Marmara Sea (McHugh et al., 2006), the Canadian margin, (Tripsanas et al., 2008), offshore Portugal (Gràcia et al., 2010), and offshore Haiti (McHugh et al., 2011). Additionally, seismically triggered turbidites have been investigated in several lacustrine settings such as Lake Washington in USA (Karlin et al., 2004), Lake Biwa in Japan (Inouchi et al., 1996; Shiki et al., 2000), Lake Zurich and Lake Lucerne in Switzerland (Schnellmann et al., 2002; Strasser et al., 2006; Anselmetti et al., 2012), as well as in several lakes of southern Chile (Bertrand et al., 2008; Moernaut et al., 2007, 2009; Moernaut, 2010).

Cascadia and northern California margins are ideal places to study turbidite paleoseismology because they have onshore paleoseismic records that can be correlated with a Holocene history of turbidites triggered by great earthquakes (Figs. 1 and 2). The onshore area of the Cascadia subduction zone margin has abundant paleoseismic evidence for rapid coastal subsidence that records buried marsh deposits and tsunami records (e.g. Atwater, 1987; Darienzo and Peterson, 1990; Atwater et al., 1995; Atwater and Hemphill-Haley, 1997; Nelson et al., 1995, 2004, 2006, 2008; Satake et al., 1996, 2003; Kelsey et al., 2002). The northern California margin, associated with the active San Andreas Fault, also has an onshore paleoseismic record based on the geodetic data and fault offset history (e.g. Prentice, 1999; Niemi and Hall, 1992; Schwartz et al., 1998; Knudsen et al., 2002; Segall, 2002; d'Alessio et al., 2005; Kelson et al., 2006; Zhang, et al., 2006).

In this paper we summarize the multiple effects of great earthquakes on the Cascadia and northern California active tectonic continental margins. We outline the seismic hazards from great earthquakes, the influence on the continental

Fig. 1. Geological setting of the Cascadia active tectonic continental margin associated with the Cascadia subduction zone, which is made up of the Juan de Fuca and Gorda plates. Cascadia and northern California margins canyons, channels, 1999–2002 core locations, and main fault systems are outlined. The pathways of the major canyons are shown in blue, and the number of correlated post-Mazama and Holocene turbidites are shown in red. See an example of the Mazama ash datum in Fig. 4. Mazama ash was not present in northern Barkley Canyon cores or in the cores south of Rogue Canyon. Note location of the Juan de Fuca channel core in Fig. 4. (Figure is modified from Goldfinger et al., 2008).

margin stratigraphy and the effects of earthquake triggering and strength on turbidite lithology.

2 Geological setting and turbidite systems

2.1 Cascadia continental margin

The Cascadia continental margin overlies the subduction zone of the Gorda and Juan de Fuca plates thrusting beneath the North American plate (Fig. 1). Cascadia Basin is the abyssal seafloor off northern California, Oregon, Washington, and Vancouver Island along the subduction zone.

A wide variety of modern turbidite systems all containing correlative, synchronously triggered turbidites are found in the Cascadia Basin (Figs. 1 and 3) (Nelson et al., 2000). The Rogue Apron is an example of a small-scale (~ 5–$10\,\mathrm{km}$ diameter) base-of-slope sand-rich apron system without evident channels (Fig. 3) (Wolf and Hammer, 1999; Nelson et al., 2000). The Astoria Fan is a channelized submarine
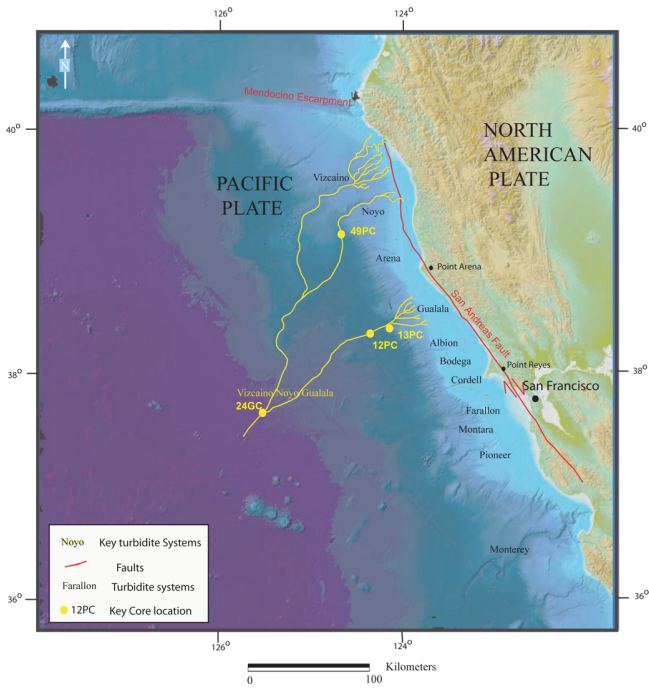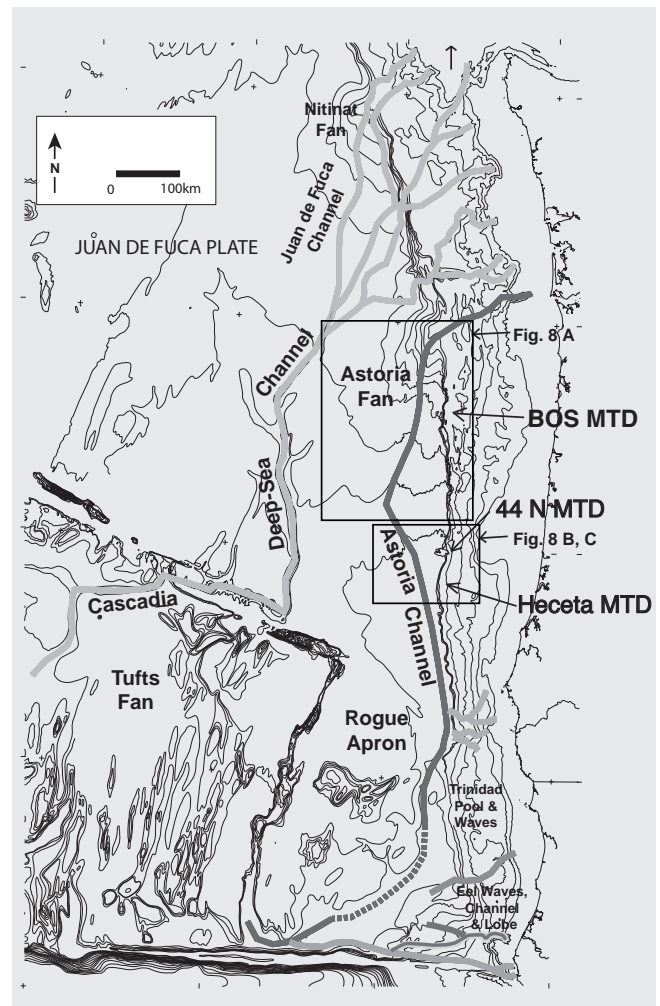
Fig. 2. Geological setting of the northern California active tectonic continental margin associated with the northern San Andreas Fault that is shown with a red line. Note location of key channels and the cores shown in Figs. 6 and 9. (Figure is modified from Gutiérrez Pastor et al., 2012).

Fig. 3. Bathymetric map showing location and setting of the BOS, Heceta, and 44 N MTDs and the different types of turbidite systems in Cascadia Basin. Nitinat and Astoria are submarine fans; Cascadia Channel is a deep-sea channel following a tectonic lineament, and Rogue Apron is a non-channelized base-of-slope apron with sheet turbidites. The Trinidad and Eel are plunge pool and sediment wave turbidite systems. The locations of Fig. 8a and b are outlined with boxes. (Figure is modified from Nelson at al., 2011).

fan that funnels sediment into depositional lobes. Cascadia Channel is a deep-sea channel system fed by multiple tributary canyons, and extends for hundreds of kilometers across Cascadia Basin. Plunge pools and dune fields associated with canyon mouths such as those of the Trinidad and Eel systems are other atypical turbidite systems (Fig. 3) (Nelson et al., 2000).

2.2 Northern California continental margin

Along the continental margin of northern California, the San Andreas Fault extends from San Francisco, where the fault parallels the coast, and then further north underlies the margin until the Mendocino Triple Junction (Fig. 2). Along the northern California margin, there are numerous canyon/channel systems containing earthquake-triggered synchronous Holocene turbidites. From the north, beginning at Cape Mendocino, to the south at Monterey Bay, the canyons and channels are Gorda, Viscaino, Noyo, Arena, Gualala, Albion, Bodega Cordell, Farallon, Montara, Pioneer and Monterey (Fig. 2) (Goldfinger et al., 2003a). The turbidite channels join together creating downstream confluence pathways. Noyo Channel, which is found south of Cape Mendocino, extends seaward for more than 200 km from the mouth of the canyon where it has a confluence with Viscaino and Gualala Channels (Fig. 2). Southern Point Arena

and Gualala canyons join at the base of the continental slope to form a channel that extends 100 km until its confluence with Noyo and Viscaino Channels. Similarly, north of the Noyo Channel, the Viscaino channel is formed by multiple tributaries that meet to develop the main channel traveling more than 200 km until a confluence with Noyo, Gualala and Cordell.

3 Methods

For paleoseismic studies, cores were recovered from all the turbidite systems along the Cascadia and northern California

margins. The core locations were selected carefully in channel pathways integrating all available swath bathymetry and archive cores in a GIS database. This allowed exploration in real time of the ocean floor and channel systems using bathymetry, backscatter data, and interactive fly-throughs of the channel morphology. Core sites were chosen to take advantage of known depositional segments of channels versus non-deposition or erosional segments to capture the most complete turbidite record.

We have investigated the sediment using visual core descriptions, photos, X-ray imaginary, CT scans, quantitative grain size analyses, mineralogical analysis and physical properties of high-resolution magnetic susceptibility and density (Goldfinger et al., 2003a, 2008, 2012). Our turbidite studies have focused on the correlation of turbidites triggered by earthquakes based on stratigraphic datums (Adams, 1990; Nelson et al., 2000), AMS radiocarbon ages and physical properties (Goldfinger et al., 2003a, b, 2006, 2007, 2008) and recurrence time intervals determined by both radiocarbon ages and hemipelagic sediment thickness and sedimentation rates (Gutiérrez Pastor et al., 2009).

To help the turbidite identification, a Geotek Multi-sensor Core Logger (MSCL) was used to obtain continuous measurements of physical properties (density, p-wave velocity and high-resolution magnetic susceptibility) for each core (e.g. Fig. 4). The physical property measurements and X-ray radiographs have been important proxies for grain size grading to identify individual turbidites with sandy/silty multiple pulses or stacked turbidites without hemipelagic sediment between the pulses (Goldfinger et al., 2007, 2008; Gutiérrez Pastor et al., 2012). A semi-quantitative mineralogical analysis was done with smear slides to identify the Mazama Ash Datum (7627 ± 150 cal yr BP) (Zdanowicz et al., 1999) in the Cascadia margin (Nelson et al., 2000; Goldfinger et al., 2003a, b). Standard heavy-mineral analysis techniques were used to define the sand/silt mineral provenances of tributary canyons in the northern California margin (Goldfinger et al., 2007). Between 2–3 cm of hemipelagic sediment were sampled below the base of each turbidite bed to obtain planktonic foraminifera for accelerator mass spectrometry (AMS) radiocarbon ages (Fig. 4).

Grain-size analyses for selected turbidites from both Cascadia and northern California margins were performed with a laser diffraction particle size analyser using the Beckman-Coulter procedure (Blott and Pye, 2006). These analyses were done to verify the physical properties as proxies for grain size and to distinguish individual turbidites with complex multiple pulses of coarser grain size from turbidites with simple fining-upward gradation. Also, we wanted to recognize associated grain size patterns in turbidites triggered by earthquakes compared with turbidites triggered by other mechanisms. All the lithologic log data, physical property logs, X-ray radiographs, and CT scan data, together with mineralogical and grain size analyses have been integrated to compare the sedimentologic characteristics of the turbidites.
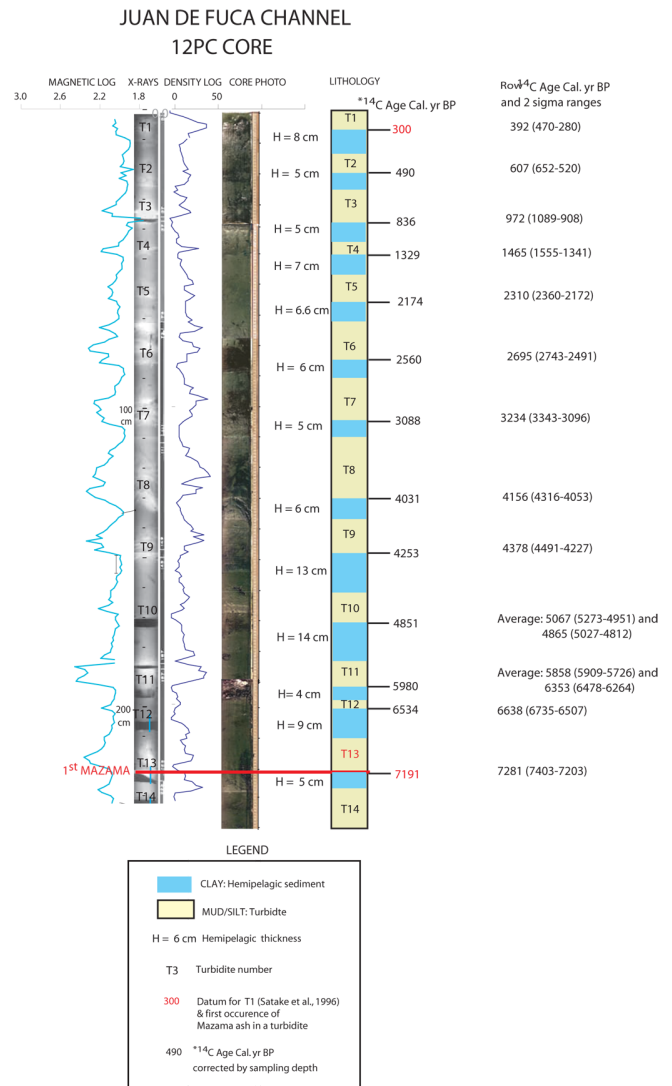
Fig. 4. Juan de Fuca Channel 12PC core showing lithology, photographs, and magnetic and density log signatures in light and dark blue, respectively. Note most turbidites have multiple coarse-grained sediment pulses in turbidites as exhibited by high density and magnetic peaks and lighter intervals in X-ray radiographs. Note that there is no hemipelagic sediment between pulses of the individual turbidites and that no mass transport deposits are evident as chaotic debris in the radiographs. The first occurrence of Mazama ash at T13, the main regional datum, is keyed in red. See Fig. 5 also for a detailed analysis of correlative turbidite characteristics. Location of Fig. 4 core is shown in Fig. 1. (Figure is modified from Gutiérrez Pastor et al., 2009).

4 Paleoseismic turbidite record

Along the Cascadia and northern California offshore margins, the paleoseismic record includes turbidites in canyon and basin floor channel turbidite systems (Figs. 1 and 2) (e.g. Nelson et al., 2000; Goldfinger et al., 2007, 2008). We and Adams (1990) have demonstrated the synchronous seismic
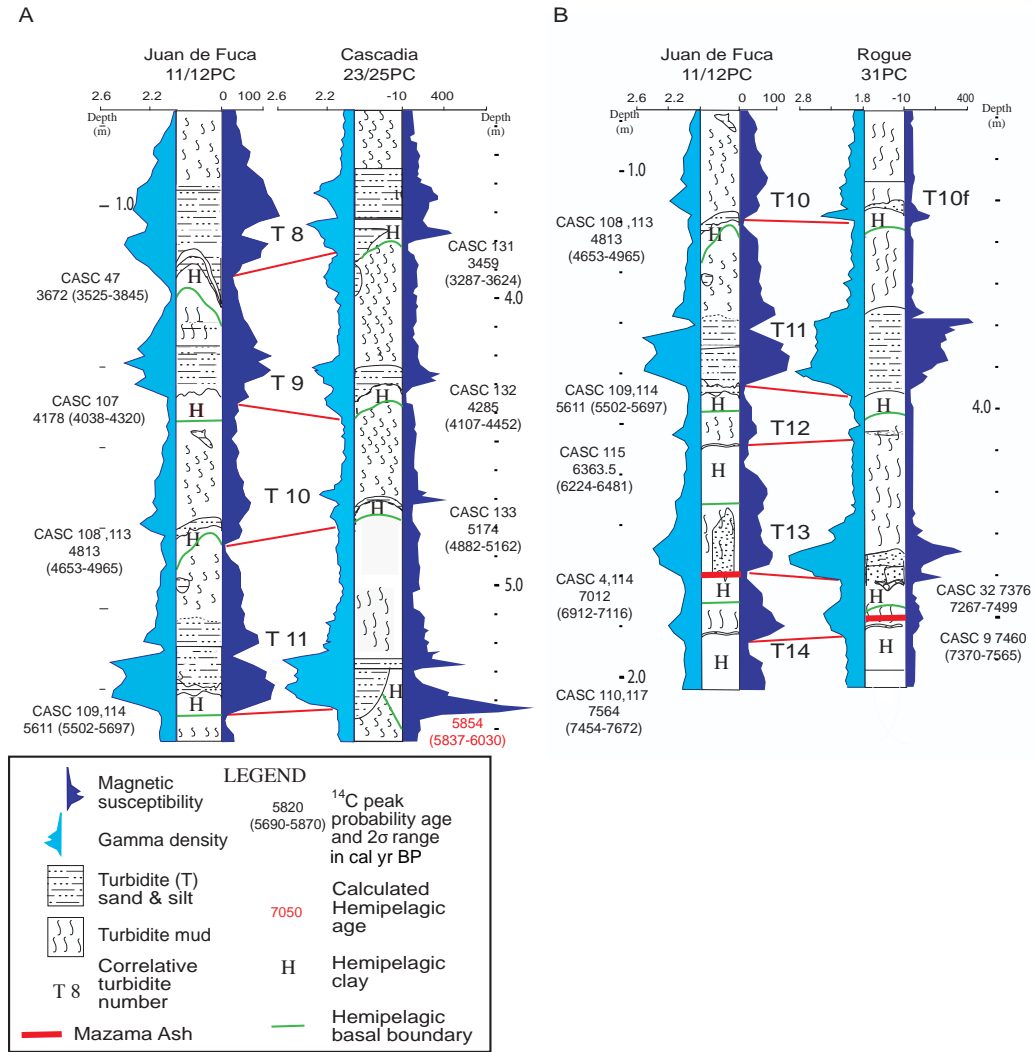
Fig. 5. An example of correlation between three piston cores: 12PC in Juan de Fuca Channel, 23PC in Cascadia Channel and 30PC in Rogue Apron. In the drawing, ¹⁴C cal yr BP ages are shown in black. Hemipelagic thicknesses are shown in the drawing with a capital H at the base of the measured thickness. Correlation of turbidites is based on number of post-Mazama turbidites, radiocarbon ages, and magnetic and density log signatures. Note the similar physical property and thickness characteristics for each correlative turbidite (e.g. T 11) found in three different turbidite system types (Juan de Fuca, Cascadia and Rogue) for 600 km along the Cascadia margin. (Figure is modified from Gutiérrez Pastor et al., 2009).

triggering of well-correlated individual turbidites from different canyon and abyssal basin channel sites for hundreds of kilometers along these active tectonic margins (Nelson et al., 2000; Goldfinger et al., 2003a, b, 2006, 2007, 2008; Gutiérrez Pastor et al., 2009). The synchroneity of turbidites in such active margins has been demonstrated through observing the same number of turbidites recorded in tributary canyons above and below confluences and by synchroneity of turbidites in different turbidite systems that are separated by hundreds of kilometers along the same margin. In previous papers, we have discussed the merits of other possible triggers for turbidity current generation such as storm wave loading, tsunamis, sediment loading, hyperpycnal flow and

aseismic accretionary wedge slip. We conclude, however, that the overwhelming evidence supports seismic triggering (Nelson et al., 2000; Goldfinger et al., 2003a, b, 2006, 2007, 2008, 2012; Gutiérrez Pastor et al., 2009).

Along the Cascadia margin, Holocene turbidites have been deposited synchronously in different channels separated by hundreds of kilometers, when turbidite deposition was not expected because the continental shelf is wider during high sea levels and the canyon heads are further from the shoreline sediment source. Great earthquakes on the subduction zone are the best candidate to explain the synchroneity of turbidite triggering in such a wide area during the Holocene time (Adams, 1990; Nelson et al., 2000; Goldfinger et al.,

2003a, b). To show synchroneity of turbidite triggering by earthquakes, the confluence test postulated by Adams (1990) utilizes the first occurrence of Mazama ash (7627 ± 150 cal yr BP) (Zdanowicz et al., 1999) in a turbidite as a marker bed; synchronous triggering is shown when the number of upstream post-Mazama ash (MA) turbidites in multiple tributaries equals the number of post (MA) turbidites downstream below the tributary confluences. In Cascadia Basin, both the Juan de Fuca and other tributary channels and the Cascadia Channel below the confluence contain 13 post-MA turbidites (Figs. 1 and 4) (Adams, 1990; Nelson et al., 2000). This test is supported by turbidite correlations based on ^{14}C ages and correlative physical properties between sample sites that are separated by several hundred kilometers along the Cascadia margin (Figs. 1, 4 and 5) (Goldfinger et al., 2003a, b, 2008, 2012).

The correlation of turbidites below the T13 post-MA turbidites has been extended so that a total of 19 Holocene turbidites can be correlated in northern Cascadia Basin (Goldfinger et al., 2007, 2008). To help extend the correlation in time, the Holocene/Pleistocene boundary has been determined by the dominance of radiolaria in the Holocene versus the dominance of foraminifera sediment in the Pleistocene sediment and by a clear change in the sediment color (Nelson, 1968, 1976 Duncan et al., 1970; Gutiérrez Pastor et al., 2009). Ages of offshore Cascadia turbidites have been demonstrated to correlate well with the onshore paleoseismic record for the past 3300 yr (Goldfinger et al., 2008, 2012).

The northern California margin also has a turbidite paleoseismic history (Fig. 2). Ages of turbidites offshore from this region have been demonstrated to correlate well with the onshore paleoseismic record even though no good datum such as the Mazama Ash or color and sediment compositional change of Pleistocene to Holocene hemipelagic sediment has been found (Goldfinger et al., 2003a, b, 2007; Gutiérrez Pastor et al., 2009). In the northern California margin, Noyo Channel has been studied in detail because its Noyo Canyon source is offset by the San Andreas Fault and thus sedimentary processes are affected directly by earthquakes associated with the canyon (Fig. 2). The channel also has an expanded Holocene turbidite record recovered from five cores containing up to 39 Holocene turbidites that can be correlated along strike (Figs. 2 and 6) (Goldfinger et al., 2007, 2008). In the Noyo Channel, as in other turbidite channels of the northern California margin, correlations have been based mainly on ^{14}C ages and stratigraphic correlation with physical property proxies (e.g. Fig. 6).

5 Hazards analysis based on turbidite recurrence times

5.1 Hazard methods background

The Cascadia and northern California continental margins contain a database of hundreds of cores and ^{14}C turbidite
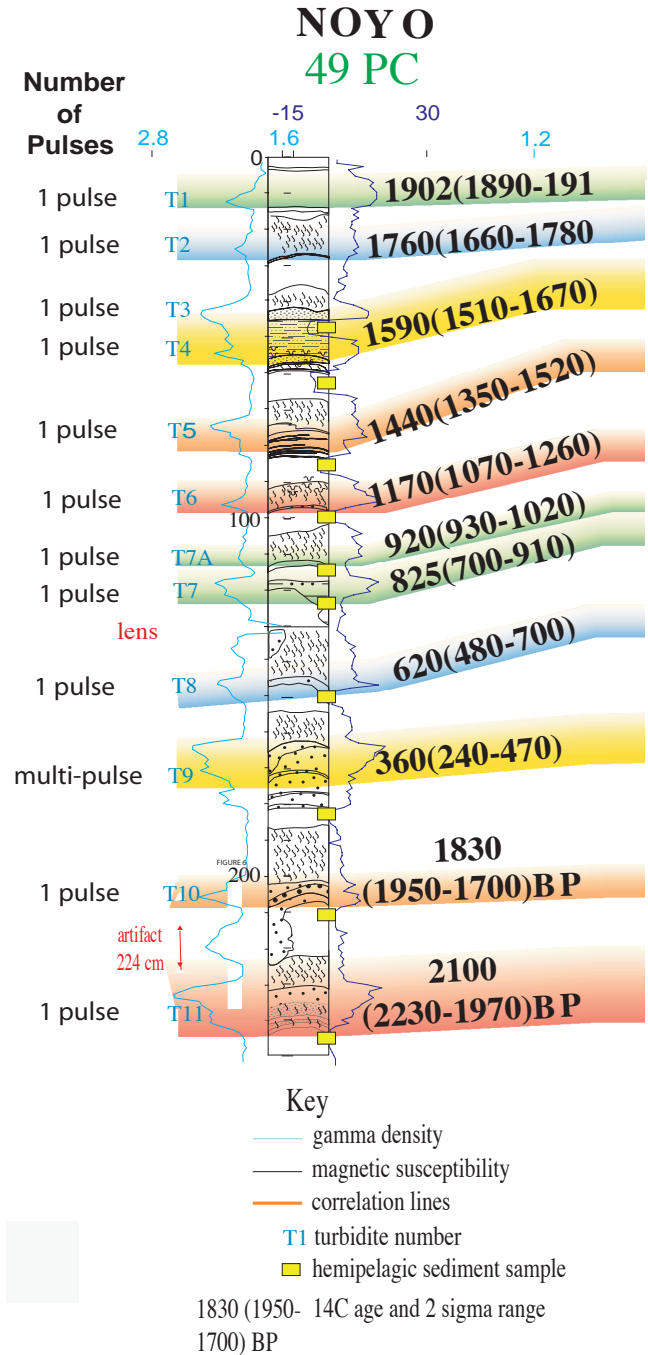
Fig. 6. Number of pulses per turbidite in Noyo Channel of the northern California margin based on physical properties and lithology. Note that we have interpreted the density signature as the most reliable proxy of grain size and these show that 11 of the first 12 turbidites in Noyo Channel are uni-pulsed. Ages for the first 9 turbidites are years AD and for turbidites 10 and 11 are calibrated radiocarbon years BP (Figure is modified from Goldfinger et al., 2007).

ages (e.g. Figs. 4 to 6) (e.g. Goldfinger et al., 2008, 2012). Our studies have shown that the evaluation of hemipelagic thickness and sedimentation rates together with ^{14}C ages can be an effective method to improve the temporal turbidite history of a continental-margin system (Gutiérrez Pastor et al., 2009). These data are of particular importance where accurate assessment of recurrence-interval statistics is integrated into assessments of seismic hazards (Goldfinger et al., 2011, 2012).

On the Cascadia subduction zone and northern California continental margins, we define and compare Holocene ages, frequency, and recurrence interval between turbidites with two methods: (1) absolute dating (^{14}C method) and (2) relative dating, based on the hemipelagic sediment thickness between two turbidites (H method) (e.g. Figs. 4 to 6) (Gutiérrez Pastor et al., 2009). We calculate turbidite recurrence times based on ^{14}C ages by determining the time difference between each pair of turbidites. Recurrence times based on hemipelagic sediment thickness are calculated by using the most reliable hemipelagic thickness based on multiple cores at a location and dividing by the moving-average sedimentation rates for the appropriate interval. Turbidite ages and recurrences times, based on ^{14}C ages or semi-independent hemipelagic thickness, generally agree if ^{14}C ages taken from anomalously thin hemipelagic interbeds are corrected for erosion.

To utilize the H method it is important to determine (1) a detailed map of sedimentation rates throughout the basin floor and (2) whether there has been a significant amount of erosion of hemipelagic sediment on the channel floors. No uniform amount of erosion is found in the Juan de Fuca and Cascadia channels because the total Holocene hemipelagic sediment thickness (without turbidites) calculated in our cores is about equal to or more than the mapped hemipelagic sediment drape thicknesses from our research (Gutiérrez Pastor et al., 2009) and previous studies (Duncan, 1968; Nelson, 1968, 1976; Griggs, 1969; Adams, 1990).

The H method is important because (1) deep-sea sedimentation provides an independent time yardstick derived from a constant rate of hemipelagic sediment deposited between turbidites; (2) hemipelagic thickness and sedimentation rate provides a set of turbidite recurrence times and calculated ages to compare with similar ^{14}C datasets; (3) the evaluation of hemipelagic sediment thickness in multiple cores at the same site can be utilized to evaluate erosion effects, and to correct radiocarbon ages obtained from anonymously thin hemipelagic sediment, which results in better correlation of turbidites and consequent paleoseismic history along the margin; (4) hemipelagic data are available for every turbidite event from multiple cores at each site compared to a single incomplete set of radiocarbon ages at each site; (5) hemipelagic data can be used to calculate ages and recurrence times for events that cannot be dated by other methods; and (6) hemipelagic data can be used to constrain radiocarbon age distributions, particularly for (i) minimum

recurrence times that are most important for hazards analysis, and (ii) where the calibration curves result in broad probability density functions (Gutiérrez Pastor et al., 2009).

To obtain a rapid preliminary estimate of turbidite recurrence times and approximate minimum time between great earthquakes in a tectonically active margin, the H method can be used with a minimum number of ^{14}C ages to establish general hemipelagic sedimentation rates over turbidite systems (Gutiérrez Pastor et al., 2009). Then the H method can be applied to a widespread distribution of cores from turbidite systems associated with the fault zone. A caveat to this method is that, when coastal and turbidite paleoseismic records need to be correlated, both complete ^{14}C and H methods are necessary. The ^{14}C and H methods applied to turbidite paleoseismology offer time spans mostly unavailable at land paleoseismic sites and the use of two complementary methods for determining earthquake frequency.

5.2 Earthquake recurrence history of Cascadia and northern California margins

The large number of age dates from cores in Cascadia Basin along with well-constrained stratigraphic datums allows an accurate measurement of turbidite recurrence intervals. On the Cascadia subduction zone margin, great earthquake recurrence times based on the most reliable turbidite paleoseismology in the Juan de Fuca and Cascadia channels for the past 5000 yr (between T1 and T10) show maximum H method and ^{14}C method recurrence times of between ~ 1000 and 1200 yr and minimum recurrence times of ~ 300–400 yr (Fig. 7) (Gutiérrez Pastor et al., 2009). Although both types of data exhibit similar maxima and minima, the H method recurrence times display a more normal distribution with a mode of 500–600 yr compared to the ^{14}C recurrences, which have a broader distribution especially for maximum time recurrences (i.e. H method ~ 1000 yr and ^{14}C method ~ 1100 to 1200 yr). Based on the H method, we find that turbidites have occurred with an average frequency of ~ 550 yr for the past ~ 5000 yr (Gutiérrez Pastor et al., 2009). Based on the average ^{14}C age of the oldest Holocene turbidite ($9800 \pm \sim 200$ cal yr BP) and the youngest deposited in 1700 AD, we find a great earthquake recurrence of ~ 530 yr (Goldfinger et al., 2012).

Along the Cascadia margin, the onshore tsunami records at Willapa Bay, Washington, and Sixes Rivers, Oregon, show average recurrence times of great earthquakes for the past 4000 yr (533 and 529 yr, respectively) that agree quite closely with those of the turbidite paleoseismic record of the past 4000 yr (~ 520 yr) (Atwater and Hemphill-Haley, 1997; Kelsey et al., 2002; Nelson et al., 2003; Gutiérrez Pastor et al., 2009).

On the northern California margin in Noyo Channel, we have been able to obtain and to compare recurrence times based on OxCal ^{14}C ages and the H method (Gutiérrez Pastor et al., 2009). By using OxCal ^{14}C ages "overlapped" with
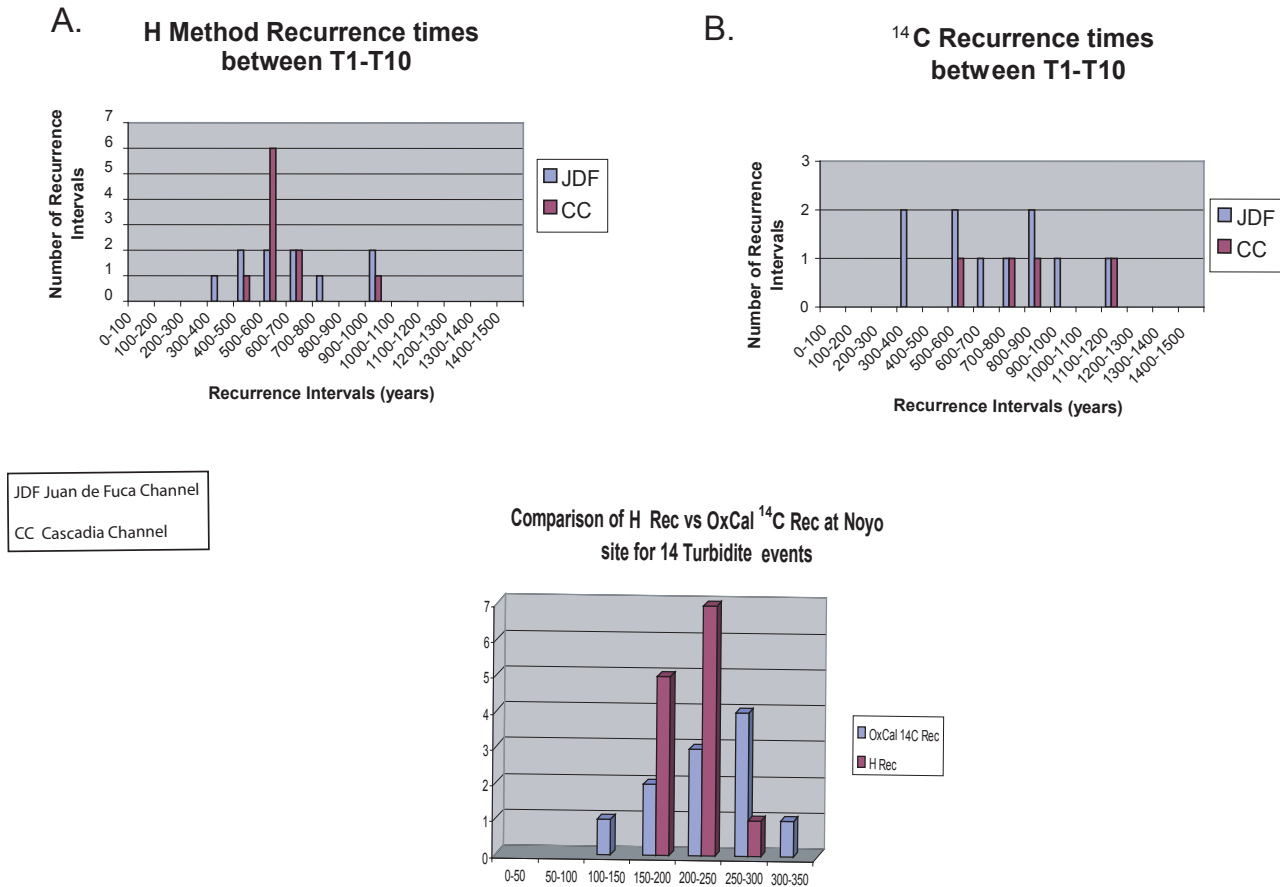
Fig. 7. (A) and **(B)** comparison of the frequency distribution of recurrences times from T1 to T10 turbidite events in Juan de Fuca (JDF) and Cascadia Channel (CC). Histogram **(A)** is based on hemipelagic sediment thickness (H Rec), and histogram **(B)** is based on AMS radiocarbon ages (^{14}C). Histograms show the number of recurrence times observed in each 100 yr interval class (e.g. 0–100 yr, 100–200 yr) at each site shown in the figure. Note that the maximum ($\sim$ 1100 to 1300 yr) and minimum ($\sim$ 300 yr) recurrence times are similar for ^{14}C and hemipelagic sediment thickness, but both extremes are more frequent for the ^{14}C dataset. Comparing both **(A)** and **(B)** histograms, we can infer that data show a major mode of recurrence times from 500 to 600 yr and a normal distribution of times, whereas the ^{14}C recurrence times are more broadly distributed. **(C)** Histogram showing the distribution of turbidite recurrence frequencies at Noyo Channel for the first 14 turbidite events based on ^{14}C ages obtained with the OxCal software and on hemipelagic sediment thickness (H Rec). We can infer that data show a major mode of recurrence times from 200 to 250 yr. Note that the H recurrence bars (H Rec) show a more normal distribution than the OxCal recurrence bars (OxCal ^{14}C Rec), with maximum recurrence times of $\sim$ 250 yr and minimum times of $\sim$ 150 yr. (Figure is modified from Gutiérrez Pastor et al., 2009).

hemipelagic analysis, we obtain better agreement in turbidite ages between H and ^{14}C methods than in Cascadia subduction zone margin, where we use cal yr BP ages. In the northern California Margin, using the H method, we obtain an average recurrence time of $\sim$ 200 yr between turbidite events, maximum times of 296 yr and minimum times of 176 yr compared to a 348 yr maximum and a 142 yr minimum recurrence times based on OxCal ^{14}C data (Fig. 7). The OxCal ^{14}C recurrence times have greater extremes than those based on the H method. Similar to Cascadia Basin, the data from California again show that the larger database of hemipelagic thickness exhibits a more normal distribution of recurrence times than the ^{14}C ages. The more normal distribution of

hemipelagic recurrence times may result in part because the database from multiple cores and all turbidites is much larger and in part because each ^{14}C recurrence value is based on two ages of the turbidite above and below, each of which can have an error. Consequently, the chances for errors with ^{14}C recurrence times are twice that compared to turbidite recurrence times based on the H method, because the two ^{14}C ages to obtain recurrence time may cause additive or subtractive ^{14}C outliers.

We observe that great earthquakes on the California margin ($\sim$ 200 yr) trigger turbidites more frequently than on the Cascadia margin ($\sim$ 500 yr), and this is corroborated by the onland record (Prentice et al., 1999; Knudsen et al., 2002;

Kelson et al., 2006; Zhang et al., 2006; Goldfinger, et al., 2007; Gutiérrez Pastor et al., 2009). At Olema, 45 km north of San Francisco, Niemi and Hall (1992) estimate that, if the 4–5 m slip event recorded in 1906 is characteristic, the recurrence time for such events would be 221 ± 40 yr. Both our data and 10 new ages from the Vedanta site and sites near Fort Ross suggest an average recurrence interval of ~ 200–230 yr (Goldfinger et al., 2007).

5.3 Hazards risk analysis

It is of great importance for hazard analysis to define accurate minimum recurrence times for great earthquakes in the Cascadia subduction zone. Because of the constant rate of hemipelagic sedimentation in channel versus inter-channel locations during the Holocene (e.g. generally 9 cm/1000 yr at Cascadia Channel), minimum ^{14}C recurrence intervals cannot be less than the stratigraphic time represented by hemipelagic sediment thickness observed in multiple cores at a location (Gutiérrez Pastor et al., 2009). For example, the minimum ^{14}C time between T1 and T2 is calculated to be 227 yr based on 5 cores in Cascadia Basin (Goldfinger et al., 2008, 2012). In contrast, six cores in Juan de Fuca and Cascadia channels contain from 4 to 8 cm (five with 5–6 cm) of hemipelagic sediment between T1-2, which equals hemipelagic recurrence times of 320 to 408 yr of stratigraphic hemipelagic sediment time (Gutiérrez Pastor et al., 2009) that must be accounted for in multiple cores. Consequently, we place the most confidence in the H method for minimum recurrence times. For the 18 turbidites in Cascadia Channel, the H method recurrence time shows one recurrence time of 221 yr that may be an outlier, but the most reliable minimum time is 278 yr (Gutiérrez Pastor et al., 2009).

On the San Andreas fault margin of California, similarly, ^{14}C minimum recurrence times are as low as 105 yr (a possible outlier), but the most reliable minimum times are 135 to 142 yr, whereas the lowest H method recurrence time is 176 yr. Consequently, at present the northern San Andreas Fault appears to be just outside the minimum recurrence time to expect a great earthquake, because the last great earthquake occurred in 1906 (Fig. 7) (Gutiérrez Pastor et al., 2009; Goldfinger et al., 2012). In contrast, the Cascadia subduction zone is within the minimum time window for a great earthquake, because the last one occurred in 1700 AD (Fig. 7) (Gutiérrez Pastor et al., 2009; Goldfinger et al., 2012).

In the southern Oregon and northern California margins of the Gorda Plate area of southern Cascadia Basin, the frequency of turbidites progressively increases towards the Mendocino Triple Junction (Fig. 1) (Nelson et al., 2000). In this region, all of the northern paleoseismic turbidites are found, as well as ~ 22 thinner turbidites of restricted latitude range that are correlated between multiple southern sites (Goldfinger et al., 2008, 2012). The northern California sites, Trinidad, Eel and Mendocino Canyons, also record additional turbidites which may be a mix of earthquake and sediment- or storm-triggered turbidites, particularly during the early Holocene when a close connection existed between these canyons and associated river systems (Nelson et al., 2000; Goldfinger et al., 2012).

The sequence of ~ 41 events defines an average recurrence period for the southern Cascadia margin of ~ 240 yr over the last 10 ka (Goldfinger et al., 2012). Time-independent probabilities range from 7–12 % in 50 yr for full or nearly full margin ruptures throughout the entire northern and southern Cascadia Basin, to ~ 21 % in 50 yr for a southern segment rupture in Cascadia Basin. Time-dependent probabilities are similar for northern margins events at ~ 7–12 %, and 37–42 % in 50 yr for the southern margin. Failure analysis suggests that, by the year 2060, Cascadia will have exceeded ~ 27 % of Holocene recurrence intervals for the northern margin, and 85 % of recurrence intervals for the southern margin.

6 Great earthquake impacts on continental margin stratigraphy

We made two important observations about active tectonic margins with great earthquakes when comparing mass transport chaotic failure deposits (MTDs) in active tectonic versus passive continental margins (Nelson et al., 2011). The first is that MTD debris flow beds are not evident in hundreds of Cascadia Basin or northern California basin floor piston cores penetrating into Late Pleistocene turbidite system deposits. (e.g. see Figs. 4 and 6). The second is that there are significantly greater amounts of MTD beds and maximum run-out distances of large MTD sheets in passive margins compared to active tectonic continental margins like the Cascadia and northern California (Table 1) (Nelson et al., 2011). The run-out of MTD flows extends only to a maximum of a few tens of kilometers onto the basin floors of the Cascadia and northern California margins (Table 1) (Figs. 3 and 8).

MTD sheets have short run-out distances of 5 to 35 km across the abyssal seafloor adjacent to the Cascadia slope even though large (65–88 km wide) and small (5–14 km wide) failure scarps and MTDs are common on the continental slope (Figs. 3 and 8) (Table 1) (Goldfinger et al., 2000; Nelson et al., 2011). These short run-out distances contrast with MTD sheets on passive margins, which can run out hundreds of kilometers across the seafloor (Table 1) (e.g. Walker and Massingill, 1970; Embley, 1976; Damuth and Embley, 1981; Simm and Kidd, 1983, 1984; Embley and Jacobi, 1986; Issler et al., 2005; Twichell et al., 2009).

The slide blocks and hummocky surfaces of the local MTD sheets are evident along the base of the Oregon slope in the swath bathymetry and GLORIA side-scan images (Fig. 8) (EEZ Scan 84 Scientific Staff, 1986; Goldfinger et al., 2000). Seismic facies and echo character from a wide variety of seismic profiles, including deep-tow side-scan sonar and 4.5 kHz seismic profiles, show the chaotic and transparent facies of
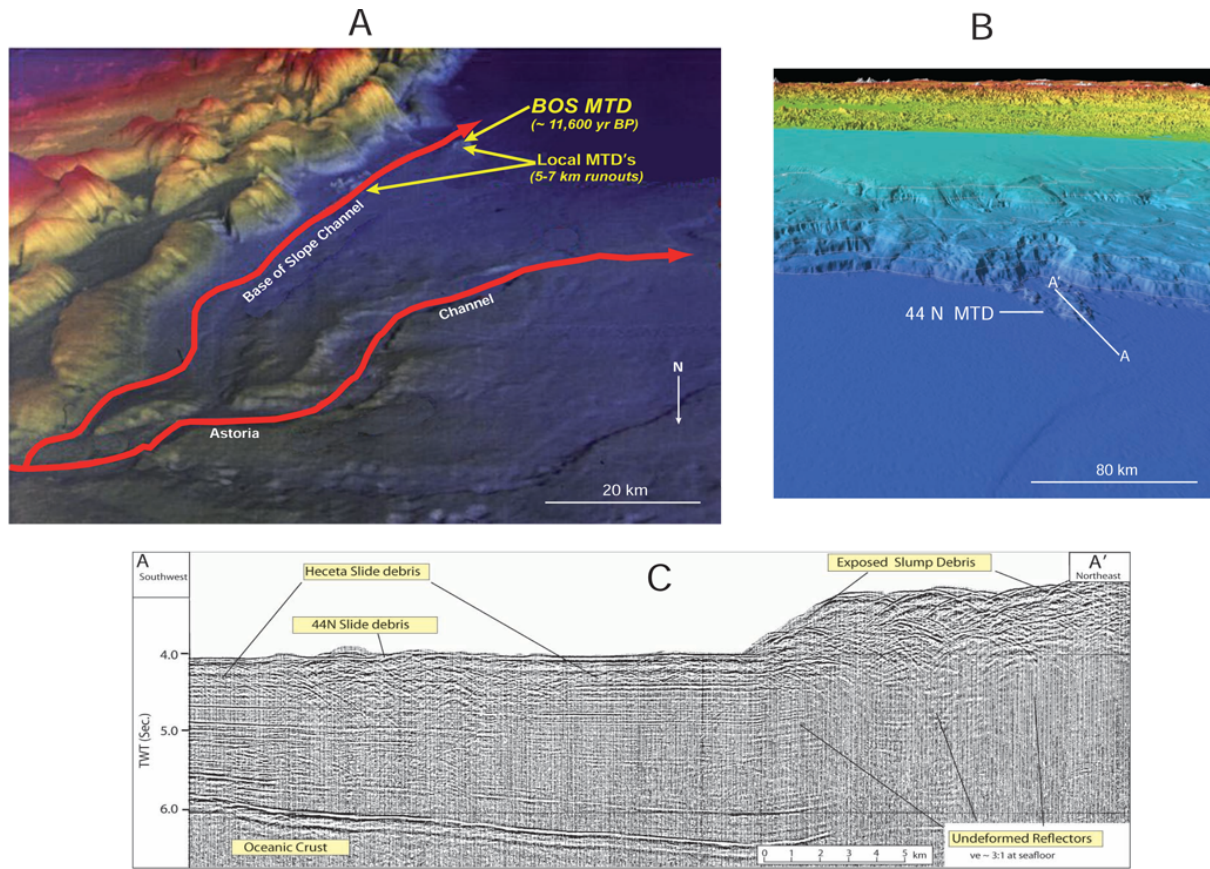
Fig. 8. (A) This 3-D swath bathymetric image looks southward from Astoria Canyon mouth over the Oregon continental slope and northern Astoria Fan. The red to yellow depth coloration highlights the shallower depths of the accretionary folds on the lower slope. The blue and brown colors highlight the channel pathways of Astoria Fan. Red lines trace the axial pathway of the Astoria Channel and base-of-slope channel, where two MTD slump debris lobes block the channel and run out about 5–7 km out from the slope base. **(B)** This 3-D swath bathymetric image looks landward towards the central Oregon continental slope and shows that the 44 N MTD (mass transport deposits) run out approximately 25 km from the slope base. **(C)** This seismic profile shows that the 44 N surface and Heceta subsurface MTDs have maximum run out distances for approximately 25 km from the base of the continental slope. The locations of **(A)**, **(B)** and **(C)** are shown in Fig. 3. (**A** is modified from Nelson et al., 2000, **B** is modified from Goldfinger et al., 2012 and **C** is from Goldfinger et al., 2000).

the MTDs (Goldfinger et al., 2000). In addition, sediment cores taken from these MTDs contain the chaotic deposits of debris flows (Fig. 8) (Goldfinger et al., 2000).

Along most of the margin from San Francisco Bay north to the Mendocino Triple Junction, few if any significant failures or MTD sheets have been identified. South from San Francisco, the Sur MTD sheet on Monterey Fan has the longest run-out distance (80 km) yet detected across an unconfined abyssal plain along any active tectonic margin (Table 1) (Normark and Gutmacher, 1988; Klauke et al., 2004; Elverhøi et al., 2005). The modern fore-arc basins off New Zealand contain MTD sheets with run-out distances of 150–200 km; however, these MTDs are found in elongate confined basins, not on the unconfined abyssal plain. Additionally, the New Zealand MTDs are fed by unusually large sediment discharge sources for an active margin (70 million mT yr^{-1}) (Lamarche et al., 2008). Active volcanoes are another

exception where MTD debris avalanches have run-outs for hundreds of kilometers (Moore et al., 1989; Weaver et al., 1995).

Other evidence supports our observations that, along the active tectonic continental margin of western North America, run-out distances of MTD sheets are limited compared to passive margins. In our studies, we observe that the active margin has MTD run-out distances of 5–80 km onto the basin floor. In a plot of selected MTD sheets from a worldwide database, the active margins have maximum run-out lengths of 80 km; in contrast, the passive margins have maximum run-out lengths of up to ~ 1000 km onto basin floors (Simm and Kidd, 1983, 1984; Issler et al., 2005), and run-outs typically are from 200 to 600 km across large passive margin submarine fans (Table 1).

We believe that the tectonic history of the Cascadia subduction zone and northern San Andreas Fault controls the

Table 1. Comparison of mass transport deposit sheets on unconfined basin floors along active and passive margins. Apparently because of seismic strengthening in active margins, maximum runout distances from the basin slope for mass transport deposits (MTDs) are up to 10 times more on passive margins. (Table is modified from Nelson et al., 2011).

Location	Max run out distance (km)	Numbers of MTDS
Active Tectonic Margin MDT sheets		
CASCADIA	5 to 35	7
North California	80	1
Issler et al. (2005)	100	45
Passive Margin MTD sheets		
Amazon Fan	140–225	4
Aleutian Basin	250–400	15
Mississippi Fan	350–600	20
Issler et al. (2005)	800	45
Simm and Kidd (1983, 1984)	1000	1

deposition of turbidites during the Holocene time and influences the character of the MTD sheets on the basin floors. Our previous studies show that there is a cyclic frequency of shaking of the continental margin by great earthquakes of approximately one every 500 yr and 200 yr for the Cascadia and California margins, respectively (e.g. Goldfinger et al., 2007; Gutiérrez Pastor et al., 2009).

Geotechnical engineers hypothesize that continental slopes of seismically active margins may develop seismic strengthening (Lee et al., 2004). This strengthening process involves gradual densification of sediment, caused by repeated earthquake events that dewater sediment. Lee et al. (2004) noted that both greater sediment strength properties measured on active-margin slopes (i.e. shear stress, consolidation) and laboratory simulations (i.e. measurements of sediment strength before and after shaking) substantiate the mechanism of seismic strengthening. Previously, studies by Lee et al. (1992) showed that denser sediment, such as that on active tectonic margins, does not mobilize as easily into debris flows as the less consolidated sediment, such as that on passive margins.

We postulate that the seismic strengthening process on active tectonic margins with great earthquakes, such as Cascadia and northern California, explains our observations that relatively short maximum run-out distances of MTD sheets on the basin floor characterize active tectonic margins, whereas the long MTD maximum run-out distances characterize passive margins (Table 1). These fundamental observations have important implications for MTD abundance and distribution in outcrop and subsurface turbidite systems of active-margin compared to passive-margin settings.

7 Great earthquake effects on turbidite lithology

The sedimentologic features of Holocene turbidites as well as the physical properties and radiocarbon ages in the active tectonic continental margin of Cascadia substantiate their seismic origin and correlation of individual turbidites at different locations throughout Cascadia Basin (Figs. 1, 4, and 5) (Nelson et al., 2000; Goldfinger et al., 2003a, b, 2006, 2007, 2008; Gutiérrez Pastor et al., 2009). Thus, we can compare the sedimentologic variations of the same turbidite from proximal to distal locations in channels. The northern California margin turbidites also are interpreted to be triggered by earthquakes based mainly on correlations of physical properties and radiocarbon ages (Figs. 1 and 6) (Goldfinger et al., 2007). Similar to Cascadia Basin turbidites, the physical property and sedimentologic characteristics of the northern California margin turbidites result from the earthquake shaking signatures and the morphology of the turbidite canyons and downstream confluences (Gutiérrez Pastor et al., 2012).

We interpret that there are two basic types of turbidites that result from triggering by great earthquakes. Because there is 96 % confidence that the physical property pulse signatures and 90 % confidence that thickness of correlated turbidites is the same upstream and downstream of channel confluences in the same turbidite system and throughout channels of all Cascadia turbidite systems, we hypothesize that the multiple pulses of individual turbidites are caused by the original seismic shaking signature of each individual great earthquake (e.g. Fig. 5) (Goldfinger et al., 2008, 2011b; Gutiérrez Pastor et al., 2012). Previous work shows that there is a predominance of multi-pulsed seismo-turbidites both upstream and downstream along channels during the Holocene along $\sim$ 600 km of the Cascadia Basin.

Stacked turbidites are a second type of seismo-turbidites that are found along the northern California margin. Unlike the Cascadia tributary canyons where there is a dominance of multi-pulsed turbidites, tributary canyons along the California margin exhibit a dominance of uni-pulsed turbidites (i.e. single fining-up classic turbidites without multiple pulses) (Fig. 6) (Gutiérrez Pastor et al., 2012). However, below confluences of tributary canyons or channels, multiple turbidity currents from synchronous earthquake triggering in these tributaries deposit stacked turbidites (Fig. 9).

Deposits of the single Gualala tributary canyon mouth (core 13PC) and Noyo tributary channel (core 49PC) compared to deposits below confluences of these tributaries (cores 12PC and 24GC) provide examples of the stacked turbidite formation processes (Gutiérrez Pastor et al., 2012). We observe that in Noyo Channel ten of the first eleven turbidites are uni-pulsed and that, in Gualala Canyon mouth, nine turbidites of the first eleven are uni-pulsed (Figs. 5 and 9) (Goldfinger et al., 2007; Gutiérrez Pastor et al., 2012). In contrast with the uni-pulsed turbidites of the Noyo and Gualala tributaries, we observe that twelve turbidites have
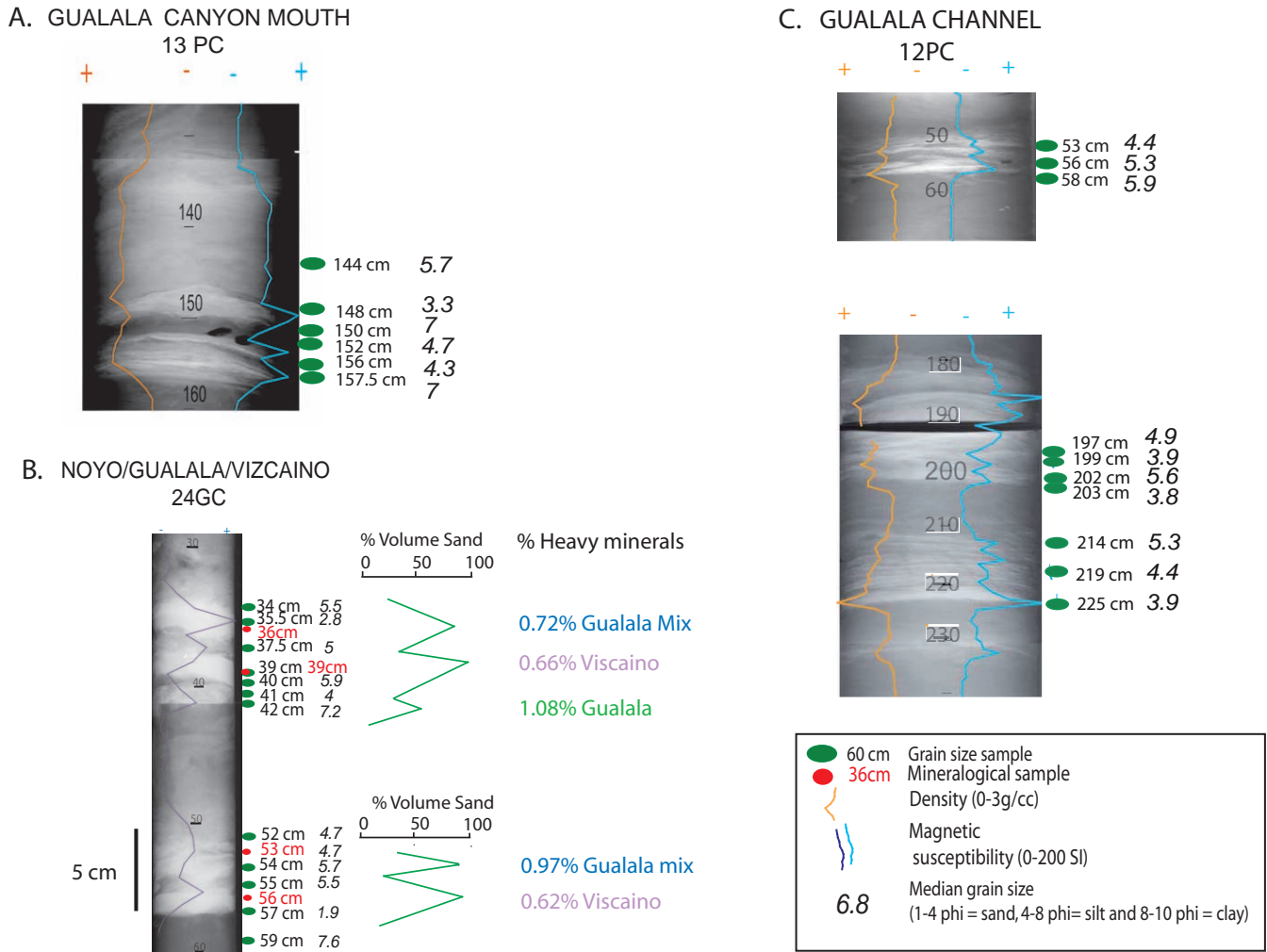
Fig. 9. Northern California margin core sections from **(A)** 13PC in Gualala Canyon mouth, **(B)** 12PC in Gualala Channel downstream from 13PC tributary site, and **(C)** 24GC below Noyo/Gualala/Vizcaino channel confluence. Core figures show X-ray radiographs, physical properties (density and magnetic signatures), grain size and mineralogy. Green dots are the grain size sample locations and numbers besides the dots are the median grain size (d50) in a phi (ϕ) scale for each sample. Red dots key mineralogic sample locations for the mineral compositions of the stacked turbidites that are shown to the right or core 24 GC. Heavy mineral compositions are a percentage of the total light and heavy mineral grains that were counted (mineralogy from Goldfinger et al., 2007). Grain-size analysis, compared with the X-ray radiography of cores and physical property logs, is used to distinguish turbidite pulses, determine presence or absence of hemipelagic sediment between pulses, and demonstrate that magnetic and density logs can be used as proxies of grain size because there is an excellent agreement between curves. Note in 13PC that two uni-pulsed turbidites are separated by 7 phi hemipelagic sediment. Note in 12PC that stacked turbidites from individual earthquake events show irregular grading of grain size and have no 7 phi hemipelagic sediment between turbidites. Note in 24GC that each stacked turbidite has a specific mineralogy correlated with different tributary canyon mineral sources. (Figure is modified from Gutiérrez Pastor et al., 2012).

multiple coarse units and two possibly are uni-pulsed 20 km downstream in the main Gualala Channel (core 12PC). Also at 12PC below the confluence of the multiple Gualala tributary canyons, as expected, we find thicker turbidites than in the 13PC tributary canyon mouth. Downstream from the confluence between Noyo, Gualala, and Vizcaino channels, single turbidite events exhibit multiple coarse-grained units (Fig. 9). The lack of hemipelagic sediment intervals between these multiple coarse-grained units shows that they deposited

during a short interval of time. Only the last coarse-grained unit has a tail, indicating final waning of a turbidity current. We interpret that these multiple coarse units are triggered by a single earthquake event because synchronous triggering in multiple tributary canyons results in the arrival of several nearly synchronous turbidity currents below the confluence of tributary canyons and channels. This is proven by the fact that each coarse unit has a distinct mineralogy from different tributary canyons and channels (Fig. 9).
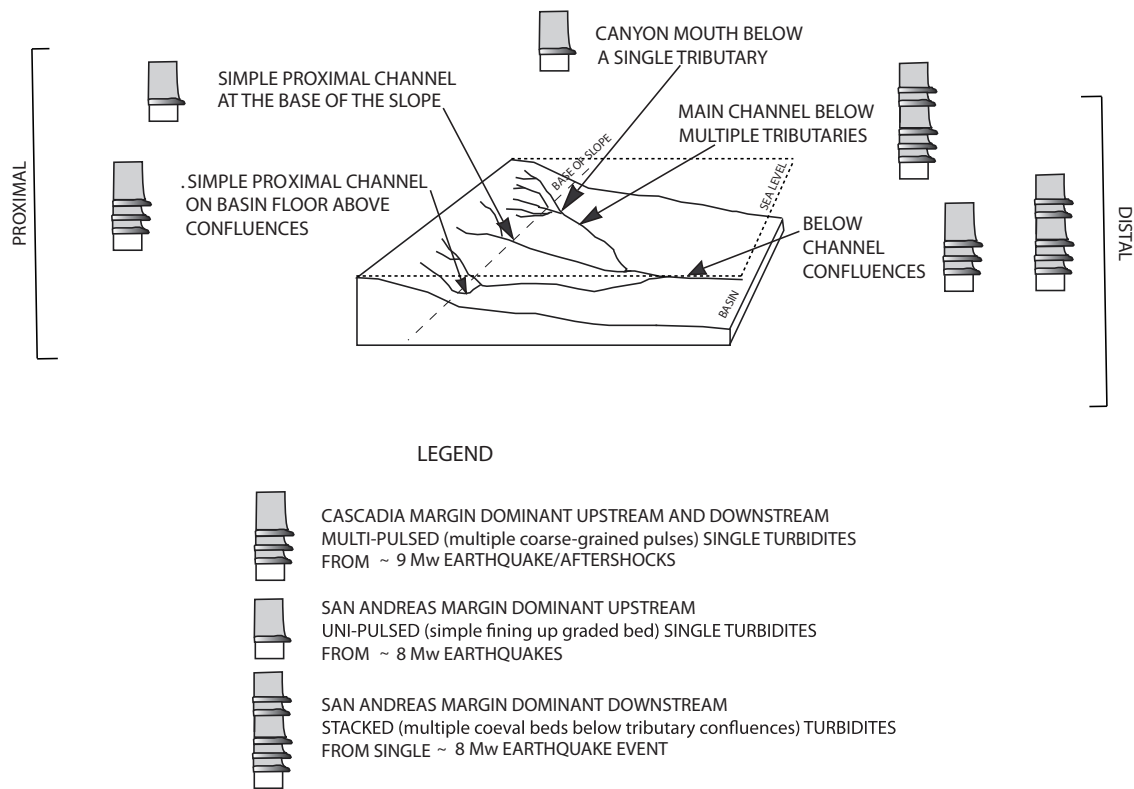
Fig. 10. Morphologic model for seismo-turbidite deposition in the active tectonic margins of western North America. Uni-pulsed, multi-pulsed or stacked turbidites are correlated with each type of canyon or channel morphologic setting and earthquake magnitude. (Figure modified from Gutiérrez Pastor et al., 2012).

The dominance of uni-pulsed turbidites in Noyo Channel and Gualala Canyon tributaries compared to the dominance of multiple coarse units in turbidites downstream in channels below tributary confluences and, most important, the different mineralogical evidence for each of the coarse units lead us to interpret that downstream these are stacked turbidites from synchronously triggered turbidity currents in multiple tributary canyons (Fig. 10). Similar turbidite characteristics have been observed in Lake Zurich, Switzerland, where multiple landslides along the lake basin walls are synchronously triggered by an earthquake and then the multiple coeval turbidity currents derived from the landslides deposit stacked turbidites on the lake basin floor (Strasser, 2006).

8   Turbidite lithology of Cascadia and California margins compared with other margins

Even though Cascadia and northern California margins have different tectonic settings, both active tectonic margins contain complex types of seismo-turbidites triggered by great earthquakes. Nearly all turbidites are multi-pulsed or stacked below canyon and channel confluences in Cascadia and California margins, although proximal uni-pulsed turbidites are dominant in Noyo Channel and Gualala Canyon (Fig. 10)

(e.g. Goldfinger et al., 2008; Gutiérrez Pastor et al., 2012). The correlative turbidites in Cascadia Basin proximal and distal channels exhibit the same mainly multi-pulsed or occasional uni-pulsed physical property signatures (Fig. 4) (Goldfinger et al., 2008, 2012; Gutiérrez Pastor et al., 2012). We interpret that the similar signatures in correlative individual turbidities throughout Cascadia Basin channels are generated by the original earthquake and/or aftershock shaking of the strongest earthquakes ($M_w \sim 9$). Generally in turbidite systems throughout Cascadia Basin, uni-pulsed turbidites are also the thinnest (Goldfinger et al., 2003, 2012), which suggests that proximal turbidites from the weakest earthquakes may not develop multiple pulses (Gutiérrez Pastor et al., 2012). In summary, in Cascadia Basin the dominantly multi-pulsed seismo-turbidites result from original great earthquake shaking and aftershocks (Fig. 10); however, occasional weaker earthquakes result in uni-pulsed turbidites upstream and downstream.

The dominance of uni-pulsed turbidites in proximal canyons and tributary channels of the California margin suggests that most of the California earthquakes are weaker than those generating the typical multi-pulsed turbidites in the proximal canyons and channels of the Cascadia margin. Apparently, because of shorter fault rupture length and

weaker earthquakes along the northern California margin ($\sim$ 200 km rupture and earthquakes $M_w \le 8$) compared to the Cascadia subduction margin ($\sim$ 600 to 1000 km rupture length and earthquakes up to $M_w \sim 9$[1]), California turbidites are mainly uni-pulsed at proximal locations above confluences and are stacked turbidites below tributary confluences (Fig. 10) (Gutiérrez Pastor et al., 2012). This is caused by the morphology of the margin that has multiple tributary sources and channel confluences where synchronously triggered turbidity currents deposit (Figs. 2 and 10).

Nakajima and Kanai (2000) as well as Shiki et al. (2000) studied seismo-turbidites from the Japan Sea plus Lake Biwa, and Gorsline et al. (2000) analyzed turbidites from the Santa Monica and Alfonso basins, California. Nakajima and Kanai (2000) observed that turbidites triggered by earthquakes exhibit different characteristics than classic turbidites described by Bouma (1962). In active tectonic margins with strong earthquakes, Japanese scientists and Gorsline et al. (2000) found that turbidites had wide areal extent, exhibited irregular sedimentary structures, grain-size breaks/fluctuations, abrupt changes in composition within the bed, variable composition among beds and greater depositional volume than turbidites triggered by other mechanisms. Our studies confirm these observations in seismo-turbidites that have detailed stratigraphic, age and physical properties correlations along entire continental margins and throughout channels (Figs. 1, 2, 4, 5, and 9) (Gutiérrez Pastor et al., 2012). In addition, we can show proximal to distal variations in seismo-turbidites that are related to earthquake strength plus canyon and channel morphologic settings, within the same margin and between different margins. We also prove that synchronous earthquake triggering in multiple canyon heads with different mineral sources results in stacked turbidites containing different mineralogies (Figs. 9 and 10) (Goldfinger et al., 2007).

Although multi-pulsed turbidites are characteristic of the Cascadia Basin turbidite systems, they are not a unique type of seismo-turbidite. Multiple pulses with inverse grading, within an individual turbidite, have been interpreted to characterize turbidites from hyperpycnal flows (i.e. hyperpycnites) (Mulder et al., 2003). Outcrops of inner levees along thalwegs of turbidite channels and along mini-basin margins also exhibit multi-pulsed turbidites (e.g. Kane and Hodgson, 2011; Kneller and MacCaffrey, 2003). Consequently, multi-pulsed turbidites are not a unique criteria for hyperpycnites, seismo-turbidites, levee turbidites, or mini-basin margins impacted by seiches or reflected turbidity currents.

The classic literature of turbidites explains the amalgamation of turbidite beds as the result of the erosion of a later separate following turbidity current. Sequential turbidity currents may erode into the previous turbidite deposits result-

ing in an amalgamated turbidite with one or several beds truncated by the erosion of different turbidity currents that follow years to hundred of years later. We show that synchronous multiple turbidity currents from different tributary canyons that are triggered by an earthquake travel thorough the confluences of tributary canyons or channels and arrive at slightly different times to deposit stacked turbidites at the same downstream site. These stacked turbidites, as well as multi-pulsed turbidites, create another type of amalgamated bed that is generated by a single earthquake event (Gutiérrez Pastor et al., 2012).

In comparison to active tectonic margins, turbidites in passive muddy margins appear to be mainly generated during low stands of sea level and by non-seismic mechanisms such as storms, floods or sediment failures resulting from overloaded and under-consolidated slope sediment (e.g. Nelson et al., 1992; Tripsanas et al., 2006; Twichell et al., 1992, 2000, 2009). The typical muddy and unstable slopes of deltaic margins off large rivers in passive margins result in combined turbidite and mass transport systems that are different from those in active tectonic margins (Nelson et al., 2011). Turbidites in passive margins appear mainly to have simple fining-upward grain size rather than mainly being multi-pulsed or stacked as they are off the active tectonic margins of western North America (Gutiérrez Pastor et al., 2012). Along the Ebro and the Mississippi deltaic margins, simple fining-upward turbidites are most common (Nelson and Maldonado, 1988; Nelson et al., 1992; Twichell et al., 2000, 2009; Nelson et al., 2009, 2011). In Bryant Canyon mini-basins, Twichell et al. (2000) and Tripsanas et al. (2006) found classic graded sand beds and muddy turbidites in the overbank deposits with the complete mud turbidite sequence of Stow and Shanmugam (1980). Although there appear to be some general differences in sedimentologic characteristics that distinguish turbidites triggered by earthquakes compared to those triggered more commonly by other mechanisms in passive margin settings, additional studies are necessary to verify these preliminary suggestions (Gutiérrez Pastor et al., 2012).

9   Conclusions

1. On the Cascadia subduction zone and northern California continental margins, we determine recurrence time interval between paleoseismic turbidites with two methods: (1) absolute dating by high-resolution AMS radiocarbon ages (^{14}C method) and (2) relative dating, based on the measure of time interval between turbidite events, using hemipelagic sediment thickness between two turbidites divided by the sedimentation rate (H method). Recurrences times, based on ^{14}C or H methods, generally agree if ^{14}C ages taken from anomalously thin hemipelagic interbeds are corrected for erosion.

---

[1]Note that an $M_w = 8$ earthquake is equivalent to 5 850 000 tons of TNT and a $M_w = 9$ eartquake is equivalent to 150 000 000 tons of TNT.

2. Great earthquakes on the northern San Andreas Fault are weaker ($M_w \sim= / < 8$) and more than twice as frequent on average (~ 200 yr) than the stronger ($M_w \sim 9$) and less frequent (~ 550 yr) earthquakes on the northern Cascadia subduction zone.

3. For the past ~ 5000 yr, the minimum recurrence times for great earthquakes are approximately 300 yr for the Cascadia subduction zone. For the past ~ 2600 yr, the minimum recurrence times for great earthquakes are approximately ~ 130 yr for the northern San Andreas Fault, which indicates both fault systems are in (Cascadia) or very close (San Andreas) to the early window for another great earthquake. Maximum recurrences times for great earthquakes are ~ 1000–1200 yr for northern Cascadia, and ~ 300–350 yr for northern San Andreas.

4. In tectonically active margins, turbidite systems are dominant and MTDs are subordinate, because great earthquakes ($M_w > 8$) cause seismic strengthening of sediment. Consequently, maximum MTD run-out distances on basin floors are an order of magnitude less (~ 100 km) in active-margin settings than in passive-margin settings (~ 1000 km). On passive margins, such as off the Mississippi River, with its high rate and amount of muddy sediment deposition, MTDs become completely intermixed with turbidite deposits at all scales from basin-wide MTD sheets (Table 1) to individual beds a few centimeters thick (Nelson et al., 2011).

5. The grain size and physical properties show that there are three characteristic types of seismo-turbidites in the Cascadia and San Andreas active tectonic margins: (1) uni-pulsed individual turbidites with simple fining-upward grain-size gradation similar to classic turbidites; (2) multi-pulsed individual turbidites with multiple coarse-grained pulses within the individual turbidite that are deposited from the same turbidity current; and (3) stacked separate turbidites that are deposited nearly synchronously from coeval turbidity currents that deposit downstream below tributary canyon or channel confluences. Both individual multi-pulsed and stacked turbidites have no hemipelagic sediment between pulses or stacked turbidites, which verifies their nearly synchronous deposition.

6. Along active tectonic margins, individual seismo-turbidites generated by the strongest great earthquakes ($M_w \sim 9$) are dominantly multi-pulsed throughout entire turbidite systems, apparently because they retain the unique shaking signature of each ($M_w \sim 9$ earthquake). Seismo-turbidites generated by the weaker great earthquakes ($M_w \sim 8$) are uni-pulsed in tributaries and become stacked turbidites in channels below tributary confluences where coeval turbidity currents deposit.

7. Multi-pulsed turbidites are not a unique criteria for seismo-turbidites, hyperpycnites (turbidites from hyperpycnal flows), or turbidites from thalweg channel levees, because multi-pulsed turbidites are found in all three depositional environments. Stacked turbidites with individual mineral pulses, however, may be unique criteria for seismo-turbidites.

8. The generation of multi-pulsed turbidites or stacked seismo-turbidites from synchronous earthquake triggering of turbidity currents in tributary canyons along active tectonic margins provides another explanation for amalgamated turbidites.

References

Adams, J.: Paleoseismicity of the Cascadia Subduction Zone: evidence from turbidites off the Oregon-Washington margin, Tectonics, 9, 569–583, 1990.

Anastasakis, G., and Piper, D.: The character of seismo-turbidites in the S-1 sapropel, Zakinthos and Strofadhes basins, Greece, Sedimentology, 38, 717-733, 1991.

Anselmetti, F., Hilbe, M., Monecke, K., Schnellmann, M., and Strasser, M.: Reconstructing recurrence rates, magnitudes and epicentral locations of strong prehistoric earthquakes, Nat. Hazards Earth Syst. Sci., submitted, 2012.

Atwater, B. F.: Evidence for great Holocene earthquakes along the outer coast of Washington State, Science, 236, 942–944, 1987.

Atwater, B. F. and Hemphill-Haley, E.: Recurrence intervals for great earthquakes of the past 3500 years at northeastern Willapa Bay, Washington, US Geological Survey Professional Paper, 1576, 1997.

Atwater, B. F., Nelson, A. R., Clague, J., Carver, G. A., Yamaguchi, D. K., Bobrowsky, P. T., Bourgeois, J., Darienzo, M. E., Grant, W. C., Hemphill-Haley, E., Kelsey, H. M., Jacoby, G. C., Nishenko, S. P., Palmer, S. P., Peterson, C. D., and Reinhart, M. A.: Summary of coastal geologic evidence for past great earthquakes at the Cascadia subduction zone, Earthquake Spectra, 11, 1–18, 1995.

Bertrand, S., Charlet, F., Chapron, E., Fagel, N., and De Batist, M.: Reconstruction of the Holocene seismotectonic activity of the Southern Andes from seismites recorded in Lago Icalma, Chile, 39°S, Palaeogeography, Palaeoclimatology, Palaeoecology, 259, 301–322, 2008.

Blott, S. J. and Pye, K.: Particle size distribution analysis of sand-sized particles by laser diffraction: an experimental investigation of instrument sensitivity and the effects of particle shape, Sedimentology, 53, 671–685, 2006.

Bouma, A. H.: Sedimentology of some Flysch Deposits, Elsevier, Amsterdam, 168 pp., 1962.

d'Alessio, M. A., Johansen, I. A., Bürgmann, R., Schmidt, D. A., and Murray, M. H.: Slicing up the San Francisco Bay Area: block kinematics and fault slip rates from GPS-derived surface velocities, J. Geophys. Res., 110, B06403, doi:10.1029/2004JB003496, 2005.

Damuth, J. E. and Embley, R. W.: Mass-transport processes on the Amazon Cone: Western Equatorial Atlantic, Am. Assoc. Petr. Geol. Bull., 65, 629–643, 1981.

Darienzo, M. E. and Peterson, C. D.: Episodic tectonic subsidence of late Holocene salt marshes, northern Oregon central Cascadia margin, Tectonics, 9, 1–22, 1990.

Duncan, J. R., Fowler, G. A., and Kulm, L. D.: Planktonic Foraminiferan-Radiolarian ratios and Holocene-Late Pleistocene deep-sea stratigraphy off Oregon, Geol. Soc. Am. Bull., 81, 561–566, 1970.

EEZ-SCAN 85 Scientific Staff: Atlas of the Exclusive Economic Zone, Gulf of Mexico and Eastern Caribbean areas: US Geological Survey, Miscellaneous Investigation Series I-1864-A, B Scale 1:500,000, Reston, Virginia, 104 pp., 1987.

Elverhøi, A., Issler, D., De Blasio, F. V., Ilstad, T., Harbitz, C. B., and Gauer, P.: Emerging insights into the dynamics of submarine debris flows, Nat. Hazards Earth Syst. Sci., 5, 633–648, doi:10.5194/nhess-5-633-2005, 2005.

Embley, R. W.: New evidence for occurrence of debris flow deposits in the deep sea, Geology, 4, 371–374, 1976.

Embley, R. W. and Jacobi, R. D.: Mass-wasting in the Western North Atlantic, in: The Geology of North America, The Western North Atlantic Region, Geological Society of America, Decade of North American Geology, edited by: Vogt, P. R. and Tucholke, B. E., Volume M, 479–490, 1986.

Goldfinger, C.: Submarine paleoseismology based on turbidite records, Ann. Rev. Mar. Sci., 3, 35–66, 2011.

Goldfinger, C., Nelson, C. H., and Johnson, J.: Holocene Earthquake records from the Cascadia Subduction Zone and Northern San Andreas Fault Based on precise dating of offshore turbidites,

Ann. Rev. Geophys., 31, 555–577, 2003a.

Goldfinger, C., Nelson, C. H., and Johnson, J. E.: Deep-water turbidites as Holocene earthquake proxies: the Cascadia Subduction Zone and Northern San Andreas Fault systems, Ann. Geofis., 46, 1169–1194, 2003b.

Goldfinger, C., Morey, A., Erhardt, M., Nelson, C.H., Gutiérrez Pastor, J., Enkin, R., and Dallimore, A.: Cascadia great earthquake recurrence: rupture lengths, correlations and constrained oxcal analysis of event ages, proceedings of the USGS Tsunami Sources Workshop, edited by: Diggles, J., Geist, E., and Lee, H., CD-ROM, 21 and 22 April, 2006.

Goldfinger, C., Morey, A., Nelson, C. H., Gutiérrez Pastor, J., Johnson, J. E., Karabanov, E., Chaytor, J., and the Shipboard Scientific Party: Rupture lengths and temporal history of significant earthquakes on the offshore and north coast segments of the Northern San Andreas, Earth Planet. Sci. Lett., 254, 9–27, 2007.

Goldfinger, C., Grijalva, K., Bürgmann, R., Morey, A.E., Johnson, J.E., Nelson, C.H., Gutiérrez Pastor, J., Ericsson, A., Karabanov, E., Chaytor, J.D., Patton, J., and Gràcia, E.: Late Holocene rupture of the Northern San Andreas Fault and possible stress linkage to the Cascadia Subduction Zone, Earth Bull. Seismol. Soc. Am., 98, 861–889, 2008.

Goldfinger, C., Nelson, C. H., Morey, A. E., Johnson, J. E., Patton, J., Karabanov, E., Gutiérrez Pastor, J., Eriksson, A. T., Gràcia, E., Dunhill, G., Enkin, R. J., Dallimore, A., and Vallier, T.: Turbidite event history – Methods and implications for Holocene paleoseismicity of the Cascadia subduction zone, US Geological Survey Professional Paper 1661–F, 184 pp., available at: http://pubs.usgs.gov/pp/pp1661f/, 2012.

Gorsline, D. S., De Diego, T., and Nava-Sanchez, E. H.: Seismically triggered turbidites in small margin basins: Alfonso Basin, Western Gulf of California and Santa Monica Basin, California Borderland, Sediment. Geol., 135, 21–35, 2000.

Gràcia, E., Vizcaino, A., Escutia, Carlota, Asioli, A., Rodés, Á., Pallàs, R., Garcia-Orellana, J., Lebreiro, S., and Goldfinger, C.: Holocene earthquake record offshore Portugal (SW Iberia): testing turbidite paleoseismology in a slow-convergence margin, Quaternary Sci. Rev., 29, 1156–1172, 2010.

Griggs, G. B.: Cascadia Channel: The anatomy of a deep sea channel: Unpublished Ph.D, Dissertation, Oregon State University, Corvallis, Oregon, 183 pp., 1969.

Gutiérrez Pastor, J., Nelson, C. H., Goldfinger, C., Johnson, J. E., Escutia, C., Eriksson, A., Morey, A. E., and Shipboard Scientific Party: Earthquake control of Holocene turbidite frequency confirmed by hemipelagic sedimentation chronology on the Cascadia and Northern California active tectonic continental margins, edited by: Kneller, B., McCaffrey, W., and Martinsen, O. J., External Controls on Deepwater Depositional Systems, SEPM Special Publication, 92, 179–197, 2009.

Gutiérrez Pastor, J., Nelson, C. H., Goldfinger, C., and Escutia, C.: Sedimentology of seismo-turbidites off the Cascadia and Northern California active tectonic continental margins, Northwest Pacific Ocean, Mar. Geol., 45 pp., 2012.

Huh, C. A., Su, C. C., Liang, W. T., and Ling, C. Y.: Linkages between turbidites in the southern OkinawaTrough and submarine earthquakes, Geophys. Res. Lett., 31, L12304, doi:10.1029/2004GL019731, 2004.

Inouchi, Y., Kinugasa, Y., Kumon, F., Nakano, S., Yasumatsu, S., and Shiki, T.: Turbidites as records of intense palaeoearthquakes

in Lake Biwa, Japan, Sediment. Geol., 104, 117–125, 1996.

Issler, D., de Blasio, F. V., Elverhøi, A., Bryn, P., and Lien, R.: Scaling behavior of clay-rich submarine debris flows, Mar. Petrol. Geol., 22, 187–194, 2005.

Kane, I. A. and Hodgson, D. M.: Submarine channel levees: nomenclature and criteria to differentiate subenvironments, Exhumed examples from the Rosario Fm. (Upper Cretaceous) of Baja California, Mexico, and the Laingsburg Fm. (Permian), Karoo Basin, S. Africa, Mar. Petrol. Geol., 28, 807–823, 2011.

Karlin, R. E., Holmes, M., Abella, S. E. B., and Sylwester, R.: Holocene landslides and a 3500-year record of Pacific Northwest earthquakes from sediments in Lake Washington, Geol. Soc. Am. Bull., 116, 94–108, 2004.

Kastens, K.: Earthquakes as a triggering mechanism for debris flows and turbidites on the Calabrian Ridge, Mar. Geol., 55, 13–33, 1984.

Kelsey, H. M., Witter, R. C., and Hemphill-Haley, E.: Plate-boundary earthquakes and tsunamis of the past 5500 yr, Sixes River estuary, southern Oregon, Geol. Soc. Am. Bull., 114, 298–314, 2002.

Kelson, K., Strieg, A., Koehler, R., and Kang, K.: Timing of Late Holocene paleoearthquakes on the Northern San Andreas Fault at the Fort Ross Orchard Site, Sonoma County, California, Bull. Seismol. Soc. Am., 96, 1012–1028, 2006.

Klaucke, I., Masson, D. G., Kenyon, N. H., and Gardner, J. V.: Sedimentary processes of the lower Monterey Fan channel and channel mouth lobe, Mar. Geol., 206, 181–198, 2004.

Kneller, B. C. and McCaffrey, W. D.: The interpretation of vertical sequences in turbidite beds: The influence of longitudinal flow structure, J. Sediment. Res., 73, 706–713, 2003.

Knudsen, K. L., Witter, R. C., Garrison-Laney, C. E., Baldwin, J. N., and Carver, G. A.: Past earthquake-induced rapid subsidence along the northern San Andreas Fault: a new paleoseismological method for investigating strike-slip faults, Bull. Seismol. Soc. Am., 92, 2612–2636, 2002.

Lamarche, G., Joanne, C., and Collet, J. Y.: Successive, large mass-transport deposits in the south Kermadec fore-arc basin, New Zealand: The Matakaoa Submarine Instability Complex: Geochem. Geophys. Geosyst., 9, Q04001, doi:10.1029/2007GC001843, 2008.

Lee, H. J., Schwab, W. C., Edwards, B. D., and Kayen, R. E.: Quantitative controls on submarine slope failure morphology, edited by: Lee, H. J., Special Issue on Marine Slope Stability, Mar. Geotechnol., 10, 143–158, 1992.

Lee, H. J., Orzech, K., Locat, J., Konrad, J. M., and Boulanger, E.: Seismic strengthening, a conditioning factor influencing submarine landslide development, 57th Canadian Geotechnical Conference, Proceedings, 8–14 [CD-ROM], 2004.

McHugh, C., Seeber, L., Cormier, M., Dutton, J., Cagatay, N., Polonia, A., Ryan, W., and Gorur, N.: Submarine earthquake geology along the North Anatolia Fault in the Marmara Sea, Turkey: A model for transform basin sedimentation, Earth Planet. Sci. Lett., 248, 661–684, 2006.

McHugh, C. M., Seeber, L., Braudy, N., Cormier, M.-H., Davis, M. B., Diebold, J. B., Dieudonne, N., Douilly, R., Gulick, S. P. S., Hornbach, M. J., Johnson III, H. E. K. R., Mishkin, C. C., Steckler, M. S., Symithe, S. J., and Templeton, J.: Offshore sedimentary effects of the 12 January 2010 Haiti earthquake, Geology, 39, 723–726, 2011.

Moernaut, J.: Sublacustrine landslide processes and their paleoseismological significance: Revealing the recurrence rate of giant earthquakes in South-Central Chile, PhD thesis, Ghent University, Belgium, 274 pp., 2010.

Moernaut, J., De Batist, M., Charlet, F., Heirman, K., Chapron, E., Pino, and M., and Brümmer, R.: Giant earthquakes in South-Central Chile revealed by Holocene mass-wasting events in Lake Puyehue, Sediment. Geol., 195, 239–256, 2007.

Moernaut, J., De Batist, M., Heirman, K., Van Daele, M., Pino, M., Brümmer, R., and Urrutia, R.: Fluidization of buried mass-wasting deposits in lake sediments and its relevance for paleoseismology: Results from a reflection seismic study of lakes Villarrica and Calafquén (South-Central Chile), Sediment. Geol., 213, 121–135, 2009.

Moore, J. G., Normark, W. R., and Holcomb, R. T.: Giant Hawaiian landslides, Ann. Rev. Earth Planet. Sci., 22, 119–144, 1994.

Mulder, T., Syvitski, J. P. M., Migeon, S., Faugeres, J. C., and Savoye, B.: Marine hyperpycnal flows; initiation, behavior and related deposits, in: Mar. Petrol. Geol., Turbidites, Models and Problems, 20, 861–882, 2003.

Nakajima, T. and Kanai, Y.: Sedimentary features of seismoturbidites triggered by the 1983 and older historical earthquakes in the easterrn margin of the Japan Sea, Sediment. Geol., 135, 1–19, 2000.

Nelson, A. R., Atwater, B. F., Brobowski, P. T., Bradley, L. A., Clague, J. J., Carver, G. A., Darienzo, M. E., Grant, W. C., Krueger, H. W., Sparks, R., Stafford, T. W., and Stuiver, M.: Radiocarbon evidence for extensive plate-boundary rupture about 300 years ago at the Cascadia subduction zone, Nature, 378, 371–374, 1995.

Nelson, A. R., Asquith, A. C., andGrant, W. C.: Great Earthquakes and Tsunamis of the past 2000 Years at the Salmon River Estuary, Central Oregon Coast, USA, BSSA, 94, 1276–1292, 2004.

Nelson, A. R., Kelsey, H. M., and Witter, R. C.: Great earthquakes of variable magnitude at the Cascadia subduction zone, Quaternary Res., 65, 354–365, 2006.

Nelson, A. R., Sawai, Y., Jennings, A. E., Bradley, L., Gerson, L., Sherrod, B. L., Sabean, J., and Horton, B. P.: Great-earthquake paleogeodesy and tsunamis of the past 2000 years at Alsea Bay, central Oregon coast, USA, Quaternary Sci. Rev. , 27, 747–768, 2008.

Nelson, C. H.: Marine Geology of Astoria Deep-Sea Fan, Ph.D. thesis, Oregon State University, Corvallis, 289 pp., 1968.

Nelson, C. H.: Late Pleistocene and Holocene depositional trends, processes, and history of Astoria Deep-Sea Fan, northeast Pacific, Mar. Geol., 20, 129–173, 1976.

Nelson, C. H. and Maldonado, A.: Factors controlling depositional patterns of Ebro turbidite systems, Mediterranean Sea, Am. Assoc. Petrol. Geol. Bull., 72, 698–716, 1988.

Nelson, C. H., Maldonado, A., Barber Jr., J. H., and Alonso, B.: Modern sand-rich and mud-rich silic-clastic aprons, alternative base-of-slope turbidite systems to submarine fans, in: Seismic Facies and Sedimentary Processes of Modern and Ancient Submarine Fans, edited by: Weimer, P. and Link, M. H., New York, Spring-Verlog, 171–190, 1992.

Nelson, C. H., Karabanov, E. B., and Colman, S. M.: Late Quaternary Lake Baikal turbidite systems, Russia, in: An Atlas of Deep-Water Environments, edited by: Pickering, K. T., Lucchi, F. R., Smith, R., Hiscott, R. N., and Kenyon, N., Chapman and

Hall, London, 29–33, 1995.

Nelson, C. H., Goldfinger, C., Johnson, J. E., and Dunhill, G.: Variation of modern turbidite systems along the subduction zone margin of Cascadia Basin and implications for turbidite reservoir beds, in: Deep-water Reservoirs of the World, Gulf Coast Section Society of Economic Paleontologists and Mineralogists Foundation 20 Annual Research Conference, edited by: Weimer, P. W., Slatt, R. M., Colman, J., Rosen, N. C., Nelson, C. H., Bouma, A. H., Styen M. J., and Lawrence, D. T., 714–738, 2000.

Nelson, C. H., Escutia, C., Goldfinger, C., Karabanov, E., and Gutiérrez Pastor, J.: External controls on modern clastic turbidite systems: three case studies, in: External Controls on Deepwater Depositional Systems, edited by: Kneller, B., McCaffrey, W., and Martinsen, O. J., SEPM Special Publication, 92, ISBN 978-1-.56576-136-0, 57-76, 2009.

Nelson, C. H., Escutia, C., Goldfinger, C., Twichell, D. C., and Damuth, J. E.: Interplay of mass-transport and turbidite-system deposits in different active tectonic and passive continental margin settings: external and local controlling factors, in: Mass Transport Deposits, edited by: Shipp, C., Weimer, P., and Posimentier, H., SEPM Special Publication, 96, 39–66, 2011.

Niemi, T. M. and Hall, N. T.: Late Holocene slip rate and recurrence of great earthquakes on the San Andreas Fault in northern California, Geology, 20, 195–198, 1992.

Noda, A., Tuzino, T., Furukawa, R., Joshima, M., and Uchida, J.: Physiographical and sedimentological characteristics of submarine canyons developed upon an active forearc slope: The Kushiro Submarine Canyon, northern Japan, Geol. Soc. Am. Bull., 120, 750–767, 2008.

Normark, W. R. and Gutmacher, C. E.: Sur submarine slide, Monterey fan, central California, Sedimentology, 35, 629–647, 1988.

Prentice, C. S., Merritts, D. J., Beutner, E. C., Bodin, P., Schill, A., and Muller, J. R.: Northern San Andreas fault near Shelter Cove, California, Geol. Soc. Am. Bull., 111, 512–523, 1999.

Satake, K., Shimazaki, K., Tsuji, Y., and Ueda, K.: Time and size of a giant earthquake in Cascadia inferred from Japanese tsunami records of January, 1700, Nature, 379, 246–249, 1996.

Satake, K., Wang, K., and Atwater, B. F.: Fault slip and seismic moment of the 1700 Cascadia earthquake inferred from Japanese tsunami descriptions, J. Geophys. Res., 108, 2535, doi:10.1029/2003JB002521, 2003.

Schnellmann, M., Anselmetti, F. S., Giardini, D., McKenzie, J. A., and Ward, S. N.: Prehistoric earthquake history revealed by lacustrine slump deposits, Geology, 30, 1131–1134, 2002.

Schwartz, D. P., Pantosti, D., Okumura, K., Powers, T. J., and Hamilton, J. C.: Paleoseismic investigations in the Santa Cruz mountains, California: Implications for recurrence of large-magnitude earthquakes on the San Andreas Fault, J. Geophys. Res., 103, 985–1018, 1998.

Segall, P.: Integratinggeologic and geodetic estimates of slip rate on the San Andreas fault system, Int. Geol. Rev., 44, 62–82, 2002.

Shiki, T., Kumon, F., Inouchi, Y., Kontani, Y., Sakamoto, T., Tateishi, M., Matsubara, H., and Fukuyama, K.: Sedimentary features of the seismo-turbidites, Lake Biwa, Japan, Sediment. Geol., 135, 37–50, 2000.

Simm, R. W. and Kidd, R. B.: Submarine debris flow deposits detected by Long range side-scan sonar 1000 km from source, Geo-Mar. Lett., 3, 13–16, 1983/1984.

Stow, D. A. V. and Shanmugam, G.: Sequence of structures in fine-grained turbidites: comparison of recent deep sea and ancient flysh sediments, Sediment. Geol., 25, 23–42, 1980.

Strasser, M., Anselmetti, F. S., Fäh, D., Giardini, D., and Schnellmann, M.: Magnitudes and source areas of large prehistoric northern Alpine earthquakes revealed by slope failures in lakes, Geology, 34, 1005–1008, 2006.

Tripsanas, E. K., Bryant, W. R., Slowey, N. C., and Kim, J. W.: Marine Isotope Stage 6 canyon and spillover deposits of the Bryant and Eastern Canyon Systems, Northwest Gulf of Mexico: importance of fine-grained turbidites on a delta-fed prograding slope, J. Sediment. Res., 76, 1012–1034, 2006.

Tripsanas, E. K., Piper, D. J. W., and Campbell, D. C.: Evolution and depositional structure of earthquake-induced mass movements and gravity flows: Southwest Orphan Basin, Labrador Sea, Mar. Petrol. Geol., 25, 645–662, 2008.

Twichell, D. C., Schwab, W. C., Nelson, C. H., Lee, H. J., and Kenyon, N. H.: Characteristics of a sandy depositional lobe on the outer Mississippi Fan from Sea MARC IA sidescan sonar images, Geology, 20, 689–692, 1992.

Twichell, D. C., Nelson, C. H., and Damuth, J. E.: Late-stage development of the Bryant Canyon turbidite pathway on the Louisiana continental slope, in: Deep-Water Reservoirs of the World, edited by: Weimer, P. W., Slatt, R. M., Colman, J., Rosen, N. C., Nelson, C. H., Bouma, A. H., Styen M. J., and Lawrence, D. T., 20th Annual GCSSEPM, CD-ROM, 1032–1044, 2000.

Twichel, D. C., Nelson, C. H., Kenyon, N., and Schwab, W.: The influence of external processes on the latest Pleistocene and Holocene evolution of the Mississippi Fan, in: External Controls on Deepwater Depositional Systems, edited by: Kneller, B., McCaffrey, W., and Martinsen, O. J., SEPM Special Publication 92, 145–157, ISBN 978-1-.56576-136-0, 2009.

Walker, J. R. and Massingill, J. V.: Slump features on the Mississippi Fan, northeastern Gulf of Mexico, Geol. Soc. Am. Bull., 81, 3101–3108, 1970.

Weaver, P. P. E., Masson, D. G., Gunn, D. E., Kidd, R. B., Rothwell, R. G., and Maddison, D. A.: Sediment mass wasting in the Canary basin, in: Atlas of Deep Water Environments, edited by: Pickering, K. T., Hiscott, R. N., Kenyon, N. H., Ricci Lucchi, F., and Smith, R. D. A., London, Chapman & Hall, 287–296, 1995.

Wolf, S. W. and Hamer, M.: Turbidite pathways in Cascadia Basin and Tufts abyssal plain, Part A, Astoria Channel, Blanco Valley, and Gorda Basin, U.S.G.S, Open File Rep. OF 99-0157, 1999.

Zdanowicz, C. M., Zielinski, G. A., and Germani, M. S.: Mount Mazama eruption: calendrical age verified and atmospheric impact assessed, Geology, 27, 621–624, 1999.

Zhang, H., Niemi, T., and Fumal, T.: A 3000-year Record of Earthquakes on the Northern San Andreas Fault at the Vedanta Marsh Site, Olema: California, Seismol. Res. Lett., 77, 248–262, 2006.